International Journal of Nanoscience
© World Scientific Publishing Company

FIELD–EFFECT TRANSISTOR STRUCTURES WITH QUASI–ONE–DIMENSIONAL CHANNEL

Slava V. Rotkin*†

Beckman Institute UIUC, 405 N.Mathews, Urbana, IL 61801, USA; Fax: (217) 244–4333

Harry E. Ruda, Alexander Shik

Energenius Centre for Advanced Nanotechnology, University of Toronto,
Toronto M5S 3E4, Canada

Received (Day Month Year)
Revised (Day Month Year)

Drift–diffusion model is applied for transport in a one–dimensional field effect transistor. A unified description is given for a semiconductor nanowire and a long single–wall nanotube basing on a self–consistent electrostatic calculations. General analytic expressions are found for basic device characteristic which differ from those for bulk transistors. We explain the difference in terms of weaker screening and specific charge density distribution in quasi–one–dimensional channel. The device characteristics are shown to be sensitive to the geometry of leads and are analyzed separately for bulk, planar and wire contacts.

Keywords: theory; nanowire/nanotube FET; drift–diffusion.

1. Introduction

In the paper we perform a study of carrier distribution and conductivity in a quasi–one–dimensional (1D) channel placed between two metal electrodes over a backgate electrode. This structure is in fact a nanowire field–effect transistor (FET) experimentally fabricated and investigated in the recent years [1,2,3] and our main task is to give an adequate theoretical description of its basic characteristics. The results can be also applied to such important object as carbon nanotube FET [4,5,6], with some restrictions due to the fact that we consider the carrier transport in the drift–diffusion model while short and clean carbon nanotubes are believed to have a ballistic conductivity [7]. That is why the theory below is presumably applicable only to long enough nanotubes. Due to a very weak screening in 1D channels, the device parameters are sensitive to the geometry of source and drain contacts and are analyzed separately for bulk, planar and 1D contacts.

*To whom correspondence should be addressed: rotkin@uiuc.edu.
†On leave from Ioffe Institute, 26 Politekhnicheskaya st., St.Petersburg 194021, Russia.

The schematic geometry of a nanowire–based FET includes the source ($x < -L/2$) and drain ($x > L/2$) electrodes connected by a nanowire of the length L and the gate electrode separated by a thin dielectric layer of the thickness d. We assume the wire to be uniformly doped with the linear concentration N. The gate voltage V_g changes the concentration in a channel controlling the FET transport. We employ the drift–diffusion model assuming that the scattering rate in the channel is sufficiently high to support a local charge equilibrium. In the opposite (ballistic) limit [7], the channel conductance has less influence on the current, which is beyond the scope of our work.

We measure all potentials from the wire midpoint ($x = 0$) so that the source and drain potentials are $\mp V_d/2$. In this case the potentials along the wire and concentration changes caused by V_g together with the contact potentials and by V_d are, respectively, even and odd functions of x and provided with the subscripts s and a: $\phi_{s,a}(x)$ and $n_{s,a}(x)$.

The potentials $\phi_{s,a}(x)$ can be divided into two parts: $\phi^0_{s,a}(x)$ created by electrodes and found from the Laplace equation containing no electron charge, and $\phi^1_{s,a}(x)$ caused by the electron charge in a wire $-en_{s,a}(x)$. We assume that the characteristic length of charge variation along the wire, $l = \min\{L, 2d\}$, exceeds noticeably the wire radius a. In this case the relationship between $\phi^1(x)$ and $n(x)$ is approximately linear [8,9,10,11] and the current j containing both drift and diffusion components can be written for a nanowire with non–degenerate carriers in the form [9]:

$$\frac{j}{e\mu} = n(x)\frac{d\phi^0}{dx} - \left[\frac{2e}{\varepsilon}\ln\left(\frac{l}{a}\right)n(x) + \frac{kT}{e}\right]\frac{dn}{dx} \tag{1}$$

where $n = n_s + n_a$, $\phi^0 = \phi^0_s + \phi^0_a$, μ is the carrier mobility, ε is the ambient dielectric permittivity. For a nanotube with $N = 0$ and degenerate carriers, kT should be replaced by the concentration–dependent Fermi energy. As a result, the square brackets in Eq.(1) are replaced by $en(x)C_t^{-1}$ with C_t being the nanotube capacitance derived in [10].

We will solve the differential equation Eq.(1) with the boundary conditions $n(\pm L/2) = n_c$ assuming the contacts to maintain constant concentration, independent of the applied voltage. Two conditions allow us to determine the integration constant and the value of current j so far considered as some unknown constant. The case $n_c = N$ corresponds to Ohmic contacts not disturbing electric properties of a wire, $n_c > N$ describes the situation where the carriers are supplied by electrodes, which is often the case for nanotubes, and $n_c < N$ corresponds to Schottky contacts. In the latter case, j is determined by the contact regions with the lowest concentration n_c determined by contacts and independent of V_g. Thus for the structures adequately described by the classical drift–diffusion theory (Eq.(1)), transconductance will be very small. The only situation of an applied interest is that when the Schottky barrier has a noticeable tunnel transparency strongly dependent on V_g. This situation has been recently considered in [7] and will not be discussed below.

2. Linear conductivity and transconductance

In the first order in V_d, Eq.(1) can be linearized in n_a and easily integrated. The knowledge of $n_a(x)$ gives us the expression for j, which becomes especially simple for $A \equiv (2e^2N/\varepsilon kT)\ln(l/a) \gg 1$ resulting in the ordinary Kirchhoffs law:

$$j = \frac{V_d}{R}, \qquad R = \frac{2}{e\mu}\int_0^{L/2}\frac{dx}{n_s}, \tag{2}$$

which is not surprising since the condition $A \gg 1$ is equivalent to neglecting the diffusion component of current. At arbitrary V_d, the described linear approach fails and determination of the whole current–voltage characteristic (CVC) $j(V_d)$ requires solution of the non–linear equation Eq.(1), which can be performed only numerically and discussed in Sec.3.

The only problem in the described linear approach consists in calculation the equilibrium concentration profile or, in other words, the potential $\phi^0(x)$. This profile and hence all the results depend noticeably on the geometry of structure, particularly, of source and drain contacts. In this section we consider bulk contacts with all three dimensions noticeably exceeding the characteristic lengths a, d, and L. Calculation of $\Phi(x, y)$, the potential created by this system of electrodes, is rather cumbersome and to obtain relatively simple analytical results, we assume additionally that the relation $d \ll L$ often realized in FETs is fulfilled is our system as well. In this case the potential distribution in the most part of inter–electrode space will not noticeably change if we neglect the dielectric–filled slit of the thickness d between the channel and the gate. In other words, we solve the Laplace equation $\Delta\Phi = 0$ in the semi–infinite strip $-L/2 < x < L/2$; $y > 0$ with the boundary conditions: $\Phi(y = 0) = V_g$; $\Phi(x = \pm L/2) = \pm V_d/2$ and then, assuming $y = d$, we obtain the $\phi^0_{s,a}(x)$. For $n_c \neq N$ it contains an additional term $\phi_c(x)$ being proportional to $(N - n_c)$ and describing the potential of uniformly charged wire [12] and derived in [9]. This gives

$$\phi^0_s(x) = \frac{8e(N-n_c)L}{\pi^2\varepsilon a}\sum_{n=0}^{\infty}\frac{(-1)^n\left\{\mathrm{K}_0\left[\frac{\pi a}{L}(2n+1)\right]-\mathrm{K}_0\left[\frac{2\pi d}{L}(2n+1)\right]\right\}}{(2n+1)^2\mathrm{K}_1\left[\frac{\pi a}{L}(2n+1)\right]}\cos\left[\frac{\pi x}{L}(2n+1)\right]$$
$$+\frac{4V_g}{\pi}\sum_{n=0}^{\infty}\frac{(-1)^n}{(2n+1)}\cos\left[\frac{\pi x(2n+1)}{L}\right]\exp\left[-\frac{\pi d(2n+1)}{L}\right]; \tag{3}$$

$$\phi^0_a(x) = V_d\left[\frac{x}{L} + \sum_{n=1}^{\infty}\frac{(-1)^n}{\pi n}\sin\left(\frac{2\pi x n}{L}\right)\exp\left(-\frac{2\pi d n}{L}\right)\right] \tag{4}$$

where K_0 and K_1 are Bessel functions of an imaginary argument.

For the linear case in the limit $A \gg 1$, Eq.(2) gives the explicit expression for the dimensionless channel conductance $\sigma = jL/(n_c e\mu V_d)$:

$$\sigma = \left[2\int_0^{1/2}\frac{dt}{1 + g\Psi(t)}\right]^{-1} \tag{5}$$

where $g = 2\varepsilon V_g/[\pi e n_c \ln(l/a)]$ and for $n_c = N$, $\Psi(t) = \sum_0^\infty \frac{(-1)^n}{(2n+1)} \cos[\pi t(2n+1)] \exp[-\pi d(2n+1)/L]$. The $\sigma(g)$ dependence has a cut–off voltage $g_0 = -\Psi^{-1}(0)$ characterized by vanishing σ. The exact behavior of σ near the cut–off can be calculated analytically. It is determined by the point of minimal concentration $x = 0$ and hence by the properties of $\Psi(t)$ at small t: $\Psi(t) \simeq \pi/2 - \arctan[\exp(-\pi d/L)] - (\pi^2 t^2/2)\sinh(\pi d/L)/\cosh^2(\pi d/L)$, which allows us to perform integration in Eq.(5) and obtain

$$i = \frac{\sqrt{(g-g_0)\sinh(\pi d/L)}}{\sqrt{2}\cosh(\pi d/L)}, \qquad g_0 = -\left\{\frac{\pi}{2} - \arctan[\exp(\pi d/L)]\right\}^{-1} \tag{6}$$

Thus the transconductance di/dg at $T = 0$ diverges at the cut–off $\sim (g - g_0)^{-1/2}$.

If $n_c \neq N$, the function $\Psi(t)$ contains additional contribution from $\phi_c(x)$. This function, studied in more detail in [9], is not analytical at $x \to \pm L/2$ but, similarly to $\phi_g(x)$, has an extremum at $x = 0$ and can be expanded in this point. This modifies the value of g_0 and the coefficient in i but retains unchanged the square–root character of $i(g)$.

The simplified expressions Eqs.(2),(5) neglect the diffusion effects, which is equivalent to the limit $T = 0$ when $n_s = 0$ for all points where $\phi_s^0(x) < -C_t^{-1} n_c$. The potential ϕ_s^0 and the carrier concentration acquire their minimal values at $x = 0$ and, hence, in the linear approximation, the cut–off voltage g_0 corresponds to the condition $\phi_s^0(0) = -C_t^{-1} n_c$ and at lower g the current is exactly zero. It is evident that at $T \neq 0$ the current at $g < g_0$ has an activation character: $j \sim \exp(-\Delta/kT)$ where $\Delta = e\left(-C_t^{-1} n_c - \phi_s^0(0)\right)$. Since $\phi_s^0(0)$ depends linearly on V_g (see, Eq.(3)), the activation energy Δ is directly proportional to $g_0 - g$. This means that the above–mentioned singularity of di/dg is fictitious and real $i(g)$ has some maximum right of g_0 with a sharp, temperature–dependent decrease at lower g.

3. Current–voltage characteristic of the channel

By measuring concentrations in units of n_c, length in units of L, potential in units of en_c/ε, and current in units of $e^2 n_c^2 \mu/(L\varepsilon)$, the basic equation Eq.(1) acquires the dimensionless form

$$j = n(x)\frac{d\phi}{dx} - \left[2\ln\left(\frac{l}{a}\right) n(x) + \tau\right]\frac{dn}{dx} \tag{7}$$

where $\tau = \varepsilon kT/(e^2 n_c)$ is the dimensionless temperature. The potential consists of three parts: $\phi(x) = \phi_c(x) + \phi_g(x) + \phi_a(x)$ describing the influence of contact work function, gate voltage and source–drain voltage and proportional, respectively, to $N - n_c, V_g$ and V_d. Their particular form depends on the geometry of contacts and for bulk contacts is given by Eqs.(3),(4). The dimensionless version of Eq.(1) for nanotubes can be easily derived from Eq.(7) by assuming $\tau = 0$ and replacing $2\ln\left(\frac{l}{a}\right) \to \varepsilon C_t^{-1}$. Eq.(7) should be solved with the boundary conditions: $n(\pm 1/2) = 1$.

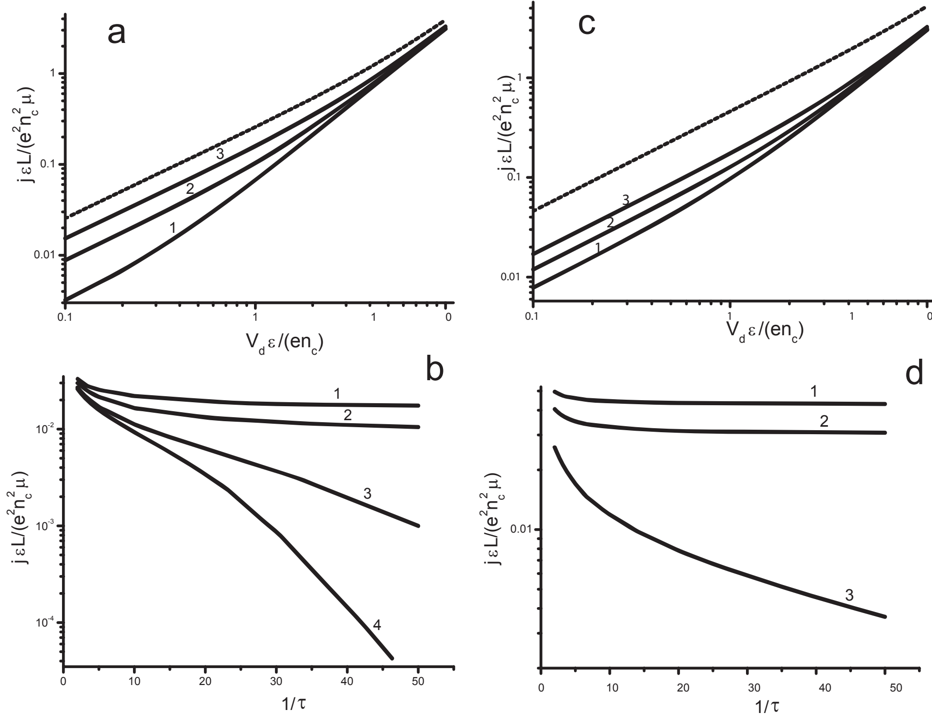

Fig. 1. Calculated characteristics of a nanowire with $d/L = 0.3$ and Ohmic contacts (a,b) and injecting contacts (c,d). (a,c) CVC for the temperatures $\tau = 0.05$ (1); 0.1 (2), and 0.2 (3): $V_g = -12$ (dashed line) and $V_g = -13.2$ (solid lines) in (a) ; $V_g = -6$ (dashed line) and $V_g = -10$ (solid lines) in (c). (b,d) Temperature dependence of linear conductance (at $V_d = 0.1$) for the same nanowire at $V_g = -12$ (1); -12.5 (2); -13 (3); -13.2 (4) in (b); -6 (1); -7.6 (2); -10 (3) in (d).

We perform numerical calculations for two situations: Ohmic contacts with $n_c = N$ and undoped nanowire (nanotube) with injecting contacts: $N = 0$. For $n_c = N$ the dimensionless threshold gate voltage $V_{g0} = (\pi g/2)\ln\left(\frac{l}{a}\right)) = -12.8$ (in units of en_c/ε) for the chosen set of parameters. Fig.1a shows CVC at two gate voltages: $V_g = -13.2$ (below the threshold) and $V_g = -12$ (above the threshold), which are superlinear because high driving voltage V_d tends to distribute carriers uniformly along the channel. In our conditions when powerful contact reservoirs fix the concentration at the points where it is maximal, such a re–distribution will increase the minimal value of n at $x = 0$ and hence increase the conductivity. Such superlinear behavior is experimentally observed in nanowire–based FETs [1,3,13,14] and differs noticeably from a sublinear CVC typical for bulk FETs and ballistic short–channel nanotube [6,15,16] structures.

Above the threshold, the channel conductivity is almost temperature–independent. The CVC curves for $V_g = -12$ (Fig.1a) at different temperatures

do not deviate from the dashed line corresponding to $\tau = 0.2$ more than by 10%. For V_g below threshold, Fig. 1a demonstrates a strong temperature dependence of the current shown in more details for $V_d = 0.1$ in Fig.1b. While the two upper curves, corresponding to above–threshold V_g, have no noticeable temperature dependence, the two lower curves demonstrate such a dependence with the activation energy growing with $|V_g|$, in accordance with the predictions of Sec.2. At high V_d, where contact injection tends to create uniform carrier concentration equal to n_c, different CVC curves merge and temperature dependence collapses.

The case of $N = 0$ formally differs from that of Ohmic contacts only by the presence of $d\phi_c(x)/dx$ in Eq.(7). As it can be seen from Eq.(3), this derivative has singularities at the contacts, which embarrasses numerical calculations. To get rid of these singularities, we use the following trick. In the closest vicinity of contacts the first term in the right side of Eq.(7) tends to infinity so that we can neglect the coordinate–independent left side. The remaining terms correspond to the quasi–equilibrium carrier distribution with ϕ_c playing the role of ϕ_s^0. This formula gives us the concentration profile in the vicinity of contacts to be matched with the solution of Eq.(7) far from the contacts. Since in this case $\phi_c(x) < 0$ (or, in other words, the electron concentration is lower due to the absence of doping), we obtain lower absolute value of the cut–off voltage V_{g0} and lower transconductance as compared to $n_c = N$. For the same parameters as above, Eq. (6) gives $V_{g0} = -7.64$. Figs.1cd present the results of numerical calculations for this case. Qualitatively they are similar to Fig.1ab but the dependencies on V_g and temperature are weaker. The above–threshold curve in Fig.1c ($V_g = -6$) is practically temperature–independent, as in Fig.1a, with the difference in currents between $\tau = 0.05$ and $\tau = 0.2$ less than 5%.

4. The role of contact geometry

The potential profile $\phi^0(x)$ and hence all FET characteristics depend on the geometry of source and drain contacts. So far we have considered bulk, three–dimensional contacts but in many cases they have not bulk but planar character representing highly conducting two–dimensional regions. In this case the profile of electric field between source and drain has singularities near contacts and differs drastically from that for bulk electrodes.

To find $\phi^0(x)$ in this case, we must solve the Laplace equation in the system of coplanar source and drain semi–planes parallel to the gate plane. The total potential created by this system consists of symmetric and antisymmetric part: $\Phi(x, y) = \Phi_s(x, y) + \Phi_a(x, y)$ obtained separately from the Laplace equations with the boundary conditions: $\Phi_s(x, 0) = V_g$, $\Phi_s(x > L/2, d) = 0$, $\frac{\partial \Phi_s}{\partial x}(0, y) = 0$ and $\Phi_a(x, 0) = 0$, $\Phi_a(x > L/2, d) = V_d/2$, $\Phi_a(0, y) = 0$. The potential along the wire $\phi^0(x) = \Phi(x, d)$.

We find $\Phi(x, y)$ with the conformal mapping $\pi z/(2d) = \ln\left(\sqrt{w} + \sqrt{w-1}\right) + \beta\sqrt{(w-1)/w}$ transforming the first quadrant at the $z = x + iy$ plane with the

cut $x > L/2$, $y = d$ into the upper semi–plane at the $w = u + iv$ plane [17] so that the source electrode corresponds to the semi–axis $u < 0$, the semi–axis $y > 0$ corresponds to the segment $0 < u < 1$ and the gate electrode corresponds to the remaining part of u–axis. The parameter β is to be found from the equation

$$\frac{L}{d} = \frac{4}{\pi}\left[\sqrt{\beta(\beta+1)} + \ln\left(\sqrt{\beta} + \sqrt{\beta+1}\right)\right] \tag{8}$$

and increases with L/d monotonically. In the (u, v) coordinate system the Laplace equation with the given boundary conditions can be easily solved:

$$\Phi_s(u,v) = V_g\left\{1 - \frac{2}{\pi}\,\mathrm{Im}[\ln\left(\sqrt{w} + \sqrt{w-1}\right)]\right\};\ \Phi_a(u,v) = \frac{V_d}{2\pi}\arctan\left(\frac{v}{u}\right). \tag{9}$$

Though we cannot transform analytically Eq.(9) into the (x, y) coordinate system and obtain $\phi^0_{s,a}(x)$ explicitly, some analytical results could be, nevertheless, obtained. The FET characteristics near the cut–off are determined by the concentration profile $n(x)$ in the vicinity of its minimum at $x = 0$. Thus we need to know only $\phi^0_s(0) \equiv \Phi_s(x = 0, y = d)$ and the second derivative of $\phi^0_s(x = 0, y = d)$ from the whole solution. In (u, v) coordinates the point $(0, d)$ corresponds to $(u_0, 0)$ where $0 < u_0 < 1$ and is determined by the equation $\arctan\sqrt{\frac{1-u_0}{u_0}} + \beta\sqrt{\frac{1-u_0}{u_0}} = \frac{\pi}{2}$. It has the asymptotes: $u_0 \simeq [\pi L/(8d)]^2$ at $L \ll d$ and $u_0 \simeq 1 - 4d^2/L^2$ at $L \gg d$. By substituting this u_0 and $v = 0$ into Eq.(9) we obtain $\phi^0_s(0)$ with the asymptotes: $\phi^0_s(0) \simeq V_g L/(4d)$ at $L \ll d$ and $\phi^0_s(0) \simeq V_g[1 - 4d/(\pi L)]$ at $L \gg d$.

Calculations of the transconductance in the linear regime are based on the same formula Eq.(5) as in Sec.2. The quantitative difference is in a particular profile of the $\Psi(t)$ function. Though its expansion near the maximum remains quadratic and hence the final result is again $di/dg = A(g - g_0)^{-1/2}$, the parameters A and g_0 may differ considerably from the case of bulk contacts. The rest of the CVC, as before, must be found by numerical calculations taking into account the fact that for two–dimensional contacts not only $\phi_c(x)$ but also $\phi_g(x)$ has singularities at $x \to \pm 1/2$ and the procedure of matching with the quasi–equilibrium solution near contacts should be used for Ohmic contacts as well.

Often (especially in the case of carbon nanotubes) contacts to 1D channel are performed with two thin wires perpendicular to its direction [18]. If these wires are infinitely long (which in fact means that their length considerably exceeds L) and have the radius a_c, then the potentials can be calculated as the sum of potentials created by 4 cylinders (source, drain and their images in the gate):

$$\phi_s(x) = V_g + \frac{V_g}{\ln(L/a_c)}\ln\frac{(x + L/2 + a_c)(-x + L/2 + a_c)}{\sqrt{4d^2 + (x + L/2)^2}\sqrt{4d^2 + (-x + L/2)^2}} \tag{10}$$

and a similar expression for $\phi_a(x)$.

5. Conclusions

We put forward a drift–diffusion model for transport calculation of FETs with a quantum wire as a channel. The unified approach allows one to apply our results

equally to the case of semiconductor nanowires and sufficiently long carbon nanotubes.

The drift–diffusion equations were written for the 1D FET and solved analytically for the linear case of small drain voltage and numerically for the rest of the CVC. We demonstrated for the first time that the week screening in 1D FETs results in a strong and interesting dependence of the device characteristics on type and geometry of the leads. We studied the cases of three-, two- and one–dimensional source and drain contacts, where some analytical solutions are possible. We presented and compared the solutions for Ohmic and injecting contacts and studied the temperature dependence of FET current at different gate voltages for these two cases.

Note added in proof. Since the paper had been written we became aware of experimental results confirming our prediction of the square root dependence of subthreshold current on the gate voltage for very long nanotube FETs. We are grateful to Prof. M. Fuhrer for sharing his data prior to publication and useful discussions.

The work of one of us (SVR) was supported in part by the Office of Naval Research grant NO0014–98–1–0604, the Army Research Office grant DAAG55–09–1–0306, the DoE Grant No. DE–FG02–01ER45932, the NSF Grant No. 9809520.

References

1. Y. Cui, X. Duan, J. Hu, and C. M. Lieber, *J. Phys. Chem. B* **104**, 5213 (2000)
2. H. Hasegawa and S. Kasai, *Physica E* **11**, 149 (2001)
3. J.-R. Kim et al., *Appl. Phys. Lett.* **80**, 3548 (2002)
4. S. J. Tans, A. R. M. Verschueren, and C. Dekker, *Nature* **393**, 49 (1998)
5. R. Martel, T. Schmidt, H. R. Shea, T. Hertel, and P. Avouris, *Appl. Phys. Lett.* **73**, 2447 (1998)
6. S. J. Wind, J. Appenzeller, R. Martel, V. Derycke, and P. Avouris, *Appl. Phys. Lett.* **80**, 3817 (2002)
7. S. Heinze, J. Tersoff, R. Martel, V. Derycke, J.Appenzeller, and Ph. Avouris, *Phys. Rev. Lett.* **89**, 106801 (2002)
8. N. S. Averkiev and A. Y. Shik, *Semiconductors* **30**, 112 (1996)
9. H. Ruda and A. Shik, *J. Appl. Phys.* **84**, 5867 (1998)
10. K.A. Bulashevich and S.V. Rotkin, *JETP Lett.* **75**, 205 (2002)
11. S. V. Rotkin, V. Srivastava, K. A. Bulashevich, and N. R. Aluru, *Int. J. Nanosci.* **1**, 337 (2002)
12. S. V. Rotkin, H. E. Ruda, and A. Shik, *Appl. Phys. Lett.***83**, 1623 (2003)
13. T. Maemoto, H. Yamamoto, M. Konami, A. Kajiuchi, T. Ikeda, S. Sasa, and M. Inoue, *Phys. Stat. Sol. (b)* **204**, 255 (1997)
14. G. L. Harris, P. Zhou, M. He, and J. B. Halpern, *Lasers and Electro–Optics, 2001, CLEO'01.* Technical Digest, p.239
15. X. Liu, C. Lee, and C. Zhou, *Appl. Phys. Lett.* **79**, 3329 (2001)
16. F. Leonard and J. Tersoff, *Phys. Rev. Lett.* **88**, 258302 (2002)
17. W. von Koppenfels and F. Stallmann, *Praxis der konformen Abbildung*, Springer–Verlag, 1959
18. J.-F. Lin, J.P. Bird, L. Rotkina, P.A. Bennett, Appl. Phys. Lett. **82** (5), 802, 2003.